[Frontiers in Bioscience E2, 627-640, January 1, 2010]

# Characterization of a novel, trastuzumab resistant human breast cancer cell line

**Mark Barok[1], Margit Balazs[2,3], Viktoria Lazar[2], Zsuzsa Rakosy[2,3], Eniko Toth[1], Andrea Treszl[2], Gyorgy Vereb[1], Gail T. Colbern[4], John W. Park[4], Janos Szollosi[1,5]**

*[1]Department of Biophysics and Cell Biology, Faculty of Medicine, Medical and Health Science Center, University of Debrecen, Debrecen, Hungary, [2]Department of Preventive Medicine, Faculty of Public Health, Medical and Health Science Center, University of Debrecen, Debrecen, Hungary, [3]Public Health Research Group of the Hungarian Academy of Sciences, University of Debrecen, Debrecen, Hungary, [4]Division of Hematology/Oncology, Department of Medicine, University of California, San Francisco, USA, [5]Cell Biology and Signaling Research Group of the Hungarian Academy of Sciences, University of Debrecen, Debrecen, Hungary*

## TABLE OF CONTENTS



## 1. ABSTRACT

HER2-positive breast cancers represent a distinct phenotype and are intrinsically more aggressive than HER2-negative tumors. Although HER2-targeted therapies have been rationally developed, resistance to these treatments represents a process understood poorly. There are few experimental models that allow studying the molecular mechanism of resistance. Our aim was to characterize a trastuzumab resistant breast cancer cell line (B585) that was established from an invasive ductal carcinoma. B585 grows only in immunodeficient mice as a xenograft. CGH and FISH were used to define cytogenetic alterations, gene-expression analysis and immunohistochemistry were applied to detect RNA and protein expression. By array-CGH focused amplifications were identified for C-MYC, EGFR, ErbB2, CCND1 and TOP2-A oncogenes. ErbB2 was co-amplified with TOP2-A. mRNA overexpression was detected for the amplified genes. ErbB2 protein was overexpressed and showed heterogeneous distribution. In summary, molecular cytogenetic analysis and expression profiling of B585 revealed several new alterations. Based on the experiments performed in SCID mice and the genotypic/phenotypic characteristics, this new *in vivo* breast cancer xenograft is a valuable model to investigate molecular mechanism of trastuzumab resistance.

## 2. INTRODUCTION

Deregulation of type I receptor tyrosine kinases (RTKs) plays a crucial role in the development of many cancers (1, 2). In humans, the widely studied type I RTKs, known also as the EGF receptor family, includes four members: ErbB-1, ErbB-2, ErbB-3 and ErbB-4. All members of the EGF family share significant homology and consist of an extracellular binding domain, a transmembrane lipophilic segment and an intracellular tyrosine kinase domain. Binding of receptor-specific ligands to ErbB-1, ErbB-3 and ErbB-4 leads to the formation of homo- and heterodimers, which result in transmission of signals controlling normal cell growth and differentiation. No soluble ligand for ErbB-2 has been identified, however, it has been shown that ErbB-2 is the preferred heterodimerization partner for ErbB-1, ErbB-3 and ErbB-4 (3-6).

Point mutation and overexpression of ErbB-2 can lead to cell transformation (7) and overexpression of ErbB-2 in breast and ovarian carcinomas correlates with poor patient prognosis (8). *In vitro* and transgenic models clearly support the hypothesis that ErbB-2 is involved in oncogenesis (9, 10). Furthermore, withdrawal of ErbB-2 in transgenic models leads to complete resolution of the breast

tumors (11). This suggests that ErbB-2 overexpressing breast cancers are driven by ErbB-2 and has lead to numerous efforts to target ErbB-2.

Trastuzumab, also known as Herceptin and rhuMAb HER2, is a humanized antibody derived from 4D5, a murine monoclonal Ab, which recognizes an epitope on the extracellular domain of ErbB2. Its addition to standard chemotherapeutic regimens is associated with high response rates and increased survival (12-15). Only ErbB2 overexpressing tumors are responsive to trastuzumab-based treatment and patients are selected using assays of protein overexpression or gene amplification. Trastuzumab is effective alone, as well as in combination with other drugs, such as taxane and vinorelbine, in many, although not all, ErBB2 positive tumors (16). For the rest of the patients the trastuzumab treatment is ineffective, although the ErbB-2 gene is amplified and the protein is overexpressed (17). This indicates that other factors must play a role in the development of primary resistance to trastuzumab and need to be identified prior to administration of therapy.

Although the mechanisms underlying the action of trastuzumab are still not fully understood, several molecular effects have been observed: ErbB2 receptor downregulation and subsequent inhibition of its downstream PI3K-Akt signaling pathway (18, 19), induction of cell cycle arrest in $G_1$ phase (20), inactivation of the mitogen-activated protein kinase and phosphoinositide-3-kinase pathways (21, 22) induction of apoptosis (23), PTEN activation (24), increase in HLA-I-restricted antigen presentation of ErbB2 (25). In addition *in vivo* models, trastuzumab decreased the microvessel density of breast cancer xenografts (26), and efficiently mediated antibody-dependent cellular cytotoxicitiy (ADCC) (27, 28).

Potential mechanisms of resistance to trastuzumab are even less understood, and thus identification of biomarkers associated with resistance would be extremely useful in optimizing treatment outcomes for HER2 positive patients. The possible mechanisms of primary or acquired trastuzumab resistance include: autocrine production of EGF related ligands (29), activation of insulin-like growth factor-I (IGF-I) receptor pathway (30), masking of the trastuzumab epitope by MUC4, a cell surface sialomucin (31, 32) or by hyaluronan (33), loss of PTEN function (24), impaired ADCC reaction (27, 34, 35).

Identification of molecular markers of potential resistance could be useful in determining non-responding patients even before start of trastuzumab treatment. While a lot of mechanisms are suspected of causing trastuzumab resistance, it is extremely important to have several models to investigate trastuzumab resistance. Furthermore, new model systems are needed, which will help to broaden our knowledge about the mechanisms of resistance, enabling us to develop drugs circumventing the trastuzumab resistance. Although trastuzumab resistant cell lines were developed from the originally trastuzumab-sensitive BT-474 cell line (36, 37), it seems important to develop cell lines which were established from the tumor of trastuzumab resistant patients. To the best of our knowledge to this time there is only one breast cancer cell line, which is a cell line of this kind (38, 39). In this study we characterize an ErbB2 positive breast cancer cell line (entitled B585) derived from a cancer patient with a trastuzumab resistant tumor. The B585 cells are able to grow only in immunodefficient SCID mice and the B585 xenografts are resistant to trastuzumab (40). The characterization was performed by applying immunohistochemistry, fluorescence *in situ* hybridization (FISH), chromosomal and array comparative genomic hybridization (cCGH and aCGH) and gene expression analysis using Affymetrix microarray platform. In addition to the overexpression of the ErbB2 protein, both integrin beta 1 and CD44 were overexpressed on B585 cells similarly to that observed on JIMT-1 trastuzumab resistant cell line. The B585 model may provide a suitable system to investigate the role of integrin beta 1 and CD44 in the trastuzumab resistance, especially in the resistance against trastuzumab-mediated ADCC.

## 3. MATERIALS AND METHODS

### 3.1. Patient clinical history

The primary breast cancer tissue used to develop the B585 xenograft was originated from a 63 year-old patient, who later developed metastasis and the patient metastatic disease was clinically resistant to trastuzumab treatment and chemotherapy. The tumor was estrogen receptor negative and ErbB2-positive high grade invasive ductal breast cancer. The patient underwent surgery with radical mastectomy and axillary lymph node evacuation (40). Approval to use the tumor cells for further investigation was obtained from the patient and local Ethical Committee prior to the initiation of cell culture.

### 3.2. Maintaining the B585 primary breast cancer xenografts in SCID mice

The B585 cells can be kept alive only *in vivo* as breast cancer xenograft in immunodeficient mice, but cannot be serially passaged *in vitro* as we described earlier (40). Tumor xenografts were harvested from donor mice, finely minced under sterile conditions, washed twice in cold Hanks' buffer, and approximately 200 micrograms of tumor tissue in 200 microliters Hanks' buffer mixed with equal volume of Matrigel (BD Matrigel, BD Biosciences, USA) was injected subcutaneously into the recipient, seven week-old female SCID C.B-17 scid/scid (originated from the laboratory of Fox Chase Cancer Center, Philadelphia, PA, USA) mice using a 18-gauge needle. The mouse population was housed in a pathogen-free environment. Only nonleaky SCID mice with murine IgG levels below 100 nanograms/mililiter were used in this study (41). Mice were monitored daily for general health. Tumor volumes were derived as the product of the length, width, and height of the tumor measured once a week with a caliper. Fifty days after inoculation the tumors started to grow and by day 90 the animals had to be euthanized because of the large tumor size. Tumor samples were collected for further analysis and the remaining tumor was transplanted into new animals.

Animals were euthanized by $CO_2$ inhalation. The animal experiments were done with the approval of the Ethical Committee of the University of Debrecen.

### 3.3. Antibodies

The anti ErbB1 monoclonal antibody (mAb) 528 (IgG2a) was produced by the hybridoma cell line 528 (HB-8509, ATCC, Manassas, VA), the anti heavy chain of human class-I HLA A, B, and C mAb (W6/32) by hibridoma cell line W6/32 (kind gift of Francis Brodsky, University of California San Francisco, USA), the anti-integrin beta 1 mAb TS2 (IgG1) by the hybridoma cell line TS2/16.2.1 (HB-243, ATCC, Manassas, VA), the anti CD44 mAb Hermes-3 by the hybridoma cell line HB-9480 (ATCC, Manassas, VA). 528, TS2 and Hermes-3 antibodies were purified using protein A affinity chromatograpy. The anti ErbB2 mAb trastuzumab (Herceptin®) (IgG1) was purchased from Roche Ltd. (Budapest, Hungary). The mouse anti human epithelial specific antigen (ESA) (also known as EpCAM (epithelial cell adhesion molecule)) mAb (mouse IgG1) was obtained from Serotec (MCA1870; Serotec, UK). Alexa647-goat-anti-mouse IgG (GAMIG, H+L) was obtained from Molecular Probes (Eugene, Oregon, USA).

### 3.4 Conjugation of antibodies with fluorescent dyes

Covalent binding of AlexaFluor 488, AlexaFluor 546 and AlexaFluor 647 succinimidyl ester (Molecular Probes, Eugene, Oregon, USA) to the primary antibodies was carried out according to the manufacturer's instructions. The dye/protein labeling ratio was approximately 3:1.

### 3.5. Immunohistochemistry

Subcutan tumors were removed from anesthetized mice, covered with Shandon Cryomatrix (Thermo Electron Corporation, USA), and stored in liquid nitrogen. 20 micrometers thick cryosections were cut using a SHANDON AS-620E Cryotome (Thermo Electron Corporation, USA) on silanized slides. Samples were fixed in 4% formaldehyde for 30 minutes and were washed twice in PBS with 1% bovine serum albumin (BSA; pH, 7.4) for 20 minutes at room temperature. Slides were labeled with a saturating concentration (10–20 micrograms/mililiter) of dye-conjugated antibodies in 100 microliters PBS containing 1% BSA overnight on ice, washed twice with PBS. When indirect labeling scheme was used, cells were first incubated with the unlabeled primary antibody, followed by the dye-conjugated secondary antibody. Unbound antibodies were removed by washing twice with PBS. After labeling, the samples were covered with 15 microliters Mowiol (Merck Kft, Budapest, Hungary) to avoid bleaching of the fluorescent dyes.

### 3.6. Confocal microscopy

A Zeiss LSM 510 confocal laser-scanning microscope (Carl Zeiss, Göttingen, Germany) was used to image samples. AlexaFluor 488 was excited with the 488 nanometers line of an argon ion laser, and its emission was detected through a 505-530 nanometers bandpass filter. AlexaFluor 546 and AlexaFluor 647 were excited with the 543 and 633 nanometers lines of a green and a red He-Ne laser, respectively, and their emissions were measured between 560-615 nanometers and over 650 nanometers, respectively. Fluorescence images were taken as 1 micrometer optical sections using a 63x (NA=1.4) oil immersion objective.

### 3.7. Chromosomal and array comparative genomic hybridization (CGH)

Chromosomal CGH (cCGH) experiments were performed as described earlier (42). The results of hybridizations were evaluated using a digital image analysis system (ISIS, Metasystems GmbH, Altlussheim, Germany). Array CGH experiments and analysis were performed as described before (43) using Human array 3.1 array containing 2.464 overlapping bacterial artificial chromosome (BAC) (13) clones (44). Array-based CGH was performed as described by Pinkel *et al.* (45). The imaging setup and costume software were described by Pinkel *et al.* (45). Image analysis was performed using two software packages (SPOT version 1.2 and SPROC version 1.1 (46). Array validation was performed using normal human female reference DNA. Array spots with more than 0.25 $Log_2$ values were considered as gains and less than -0.25 $Log_2$ values as losses.

### 3.8. Gene expression analysis

Total RNA was isolated from freshly removed B585 tissue using RNeasy Mini kit according to the protocol of the supplier (Qiagen, GmbH, Germany). Normal breast tissues were used as control. RNA concentrations were measured using NanoDrop ND-1000 UV-Vis Spectrophotometer (NanoDrop Technologies, Wilmington, Delaware USA). The integrity of the RNA was determined on the Agilent 2100 Bioanalyser using RNA 6000 Nano Kit (Agilent Technologies, Palo Alto, CA). All samples used for gene expression analysis had a 28S/18S ribosomal RNA ratio of more than 1.5. The mRNA levels were determined using Affymetrix GeneChip Human Genome U133 Plus 2.0 expression arrays (Heidelberg, GeneCore Genomics Core Facility, Germany). Gene expression analyses were carried out using the GeneSpring 7.3 software (Agilent Technologies). Raw intensity values from each chip were normalized to the 50 percentile of the measurements taken from that chip to reduce chip-wide variations in intensity. Each gene was normalized to the average measurement of that gene to enable comparison of relative changes in gene expression levels between different conditions. Volcano plot with a p value cut off of 0.05 were applied for identification of differentially expressed genes with minimum 2-fold differences. For multiple testing corrections the Benjamini and Hochberg false discovery rate was used.

### 3.9. Correlation of aCGH and expression data

The web-based MatchMiner program (47) was applied to match the amplified FISH clone IDs of aCGH to the appropriate Affymetrix microarray probe sets. For genes that were represented by more than one probe sets on the Affymetrix array, we used the sequence that gave the highest correlation between oligonucleotide array expression data.

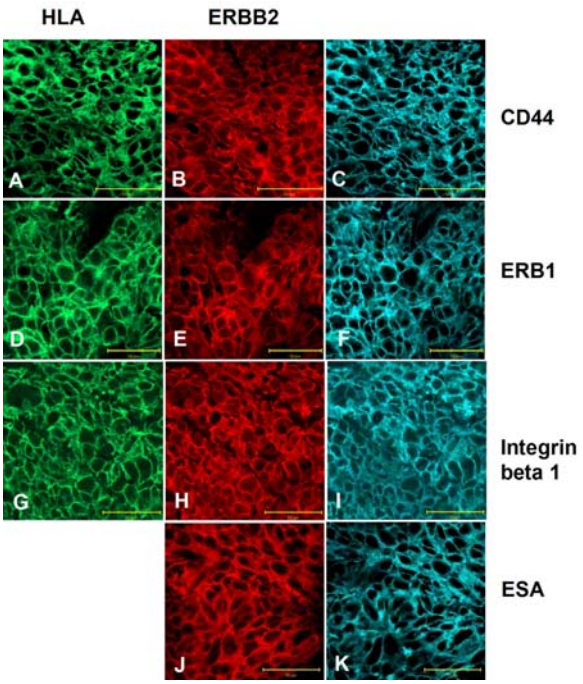


**Figure 1.** Immunohistochemical characterization of the B585 xenograft. Fast frozen sections from B585 xenografts were labeled to HLA class-I antigen (green; A, D, G), ErbB2 (red; B, E, H, J), CD44 (C), ErbB1 (F), integrin beta 1 (I) and epithelial specific antigen (ESA) (K). Images in the same row repesent the same sample which was labeled for 2 or 3 different antigens. Human epithelial specific antigen, ESA was visualized with indirect immunofluorescence using AlexaFluore 647-GAMIG as secondary antibody. To the control sample, which was labeled with only trastuzumab and GAMIG, GAMIG could bind weakly (date not shown). Images were taken with a Zeiss LSM510 laser scanning confocal microscope as described in Materials Methods.

### 3.10. Fluorescence *in situ* hybridization

For the characterization of breast cancer specific gene alterations at a single cell level double and triple labeled DNA probe sets were applied. The ProVysion multi-color probe kit consisted the centromere specific chromosome 8 (SpectrumAqua labeled), lipoprotein lipase region (LPL) (8q21.23) (SpectrumOrange labeled) and C-MYC (8q24) (SpectrumGreen labeled) (Vysis Inc. Des Plains, IL, USA). The chromosome 17 specific centromeric probe (SpectrumAqua) was cohybridized with Topoisomerase II-alpha gene (TOP2A, SpectrumOrange) and ErbB2 (SpectrumGreen) gene specific probes (Vysis Inc.). The N-MYC (2p24.1; SpectrumOrange) and the centromeric probe for chromosome 2 (Spectrum Green) as well as the EGFR (7p13; SpectrumOrange) and the centromeric 7 probe (SpectrumGreen) were hybridized simultaneously (Vysis Inc.). The 8p22 region specific probe was isolated from bacteria clones generously supplied by Molecular Genetic Resources (University of Bari, Bari, Italy). Centromere-specific probes for chromosomes 1, 2, 6-9, 11, 12, 17, 18, 20 and X were isolated from bacteria clones (University of Bari, Italy). DNA probes were labeled with biotin-dUTP by nick translation using BioNick kit, according to the protocol of the supplier (Gibco BRL, Germany). All FISH experiments were carried out as described earlier or according to the manufacturer instructions (48-50). Samples were scored for the number of fluorescent signals in each nucleus by using a fluorescence microscope (OPTON, Oberkochen, Germany) equipped with selective filters for the detection of FITC, SpectrumGreen, SpectrumOrange and DAPI. Approximately 200-500 nuclei and/or 10 metaphases were scored for each hybridization. Three-color images were captured using a digital imaging analysis system (ISIS, Metasystems GmbH, Althussheim, Germany).

## 4. RESULTS

### 4.1. Immunohistochemical characterization of the B585 xenograft

Similarly as previously reported (40) our attempts to develop *in vitro* cell culture from the B585 xenografts using different cell culture conditions were unsuccessful. The B585 cells can recover from cryopreservation, and can grow only in immunodeficient mice as xenograft and they can be bred as transplantation into new animals. Injection of B585 cells subcutaneously into SCID mice lead to formation of xenograft tumors in more than 90% of the animals tested. From the seventh week onwards, the tumors started to grow exponentially in these mice and by day 90 the animals had to be euthanized because of the large tumor size. Fast frozen tissue sections were labeled with fluorescent antibodies. Figure 1. A, D, G show the positive immunohistochemical staining of the B585 tumor cells for the HLA-I antigen. Similarly to the original primary tumor the B585 cells maintained in xenograft were intensely ErbB2-positive (Figure 1 B, E, H, J). The established xenograft cell line was also positive for CD44 (Figure 1C), ErbB1 (Figure 1F), integrin beta 1 (Figure 1I) and ESA (Figure 1K).

### 4.2. Genetic alterations in the original primary breast tumor and the B585 xenograft

To search for copy number alterations in the B585 genome, we performed chromosomal CGH analysis using DNA from both samples (patient's primary tumor and xenograft). Copy number alterations of the original tumor and the B585 cell line matched well, 24 aberrations were seen by cCGH in the original lesion and B585 xenograft as well. Common alterations involved 11 chromosomal region gains and 9 regional deletions. Alterations present in both samples included gains at 1q, 2p11.2-p15, 6p11.2-p21, 6p22-p23, 7, 10p, 11q12-q14, 12p, 16p, 18q11.2-q21, 19 and losses at 2p16-pter, 3p14-q13.3, 4p, 4q12-q21, 4q22-qter, 8p21-8pter, 13q, 14q, 15q11.2-q22.2. The cCGH data are summarized in Table 1.

In order to increase the resolution of copy number gains and losses array CGH analysis was also performed using the 1.4 MB BAC array (HumArray3.2). The array CGH results were highly concordant for regions identified by cCGH, however numerous single copy amplicons and small deletions, that were not seen by cCGH were also detected. The quality of the array CGH

**Table 1**. Summary of chromosome copy number gains and losses in the primary breast tumor and the B585 xenograft by chromosomal CGH

| Genetic alterations | Gains | Losses | Number of alterations all (gains/losses) |
|---|---|---|---|
| Common genetic alterations in both patient tumor and B585 xenograft | 1q, 2p11.2-p15, 6p11.2-p21, 6p22-p23, 7, 10p, 11q12-q14, 12p, 16p, 18q11.2-q21, 19 | 2p16-pter, 3p14-q13.3, 4p, 4q12-q21, 4q22-qter, 8p21-8pter, 13q, 14q, 15q11.2-q22.2 | 20 (11/9) |
| in B585 xenograft only | 4q12-q21, 18q22-qter | 9q ,10q | 4 (2/2) |
| in the patient tumor only | 6q23-qter, 12q22-qter | 5q12-pter, 21q | 4 (2/2) |

**Table 2.** Amplifications in the B585 genome detected by array CGH

| Clone | $Log_2$Rat | Cromosome band | Genes covered by the clone |
|---|---|---|---|
| RP11-100B16 | 2.537 | 8p12-8p11.23 | LETM2. FGFR1. DDHD2. WHSC1L1. PPAPDC1B |
| RP11-265K5 | 2.487 | 8p12 | DDHD2. WHSC1L1. LETM2. FGFR1 |
| RP11-42M12 | 2.033 | 5q23.2-q23.3 | |
| DMPC-HFF#1-71E5 | 2.001 | 8q24.21 | MYC |
| RP11-282J24 | 1.640 | 8p11.21 | ANK1 |
| RP11-48D21 | 1.561 | 8p11.21 | ZMAT4 |
| RP11-124D1 | 1.456 | 20q13.13 | PREX1 |
| GS-7N12 | 1.430 | 11q13.5-q14.1 | PAK1 |
| RP11-118F19 | 1.350 | 16q24.1 | KIAA0182. GINS2 |
| DMPC-HFF#1-61H8 | 1.346 | 17q12 | ERBB2 |
| CTD-2031K20 | 1.334 | 20q13.13 | CEBPB |
| RP11-256P19 | 1.305 | 11q13.4 | FOLR2 |
| CTD-2060E7 | 1.246 | Xq28 | AFF2 |
| RP11-168B13 | 1.222 | 11q13.4-11q13.5 | RPS3. GDPD5 |
| CTC-437H15 | 1.219 | 11q13.3 | CTTN |
| RP11-120P20 | 1.167 | 11q13.3 | SHANK2 |
| CTB-36F16 | 1.158 | 11q13.2-11q13.3 | CCND1 |
| RP11-149G19 | 1.149 | 11q13.2 | LRP5 |
| RP11-17D23 | 1.148 | 2p15 | USP34 |
| GS-274P9 | 1.147 | 2p16.1-p15 | REL |
| RP11-24P23 | 1.138 | 2p14-2p13.3 | TGFA |
| CTD-2125H12 | 1.102 | 20q13.1 | CEBPB |
| RP11-192M1 | 1.093 | 1q42.12 | TMEM63A. LEFTY1. PYCR2. LEFTY2. |
| RP11-64N21 | 1.077 | 12p11.23 | STK38L. ARNTL2 |
| RP11-24N12 | 1.071 | 12p13.33-12p13.32 | TEAD4. TSPAN9 |
| RP1-17L4 | 1.069 | 11q13.2-11q13.3 | FGF4 |
| RP11-51K19 | 1.047 | 20q13.13 | PREX1 |
| RP11-675B4 | 1.044 | 11q13.1 | SF3B2. PACS1 |
| CTC-352E23 | 1.037 | 11q13.5 | LRRC32 |
| RP11-119C13 | 1.031 | 11q13.5 | UVRAG. WNT11 |
| RP11-102M18 | 1.028 | 11q13.4 | WDR71. UCP2. UCP3 |
| RP11-17D23 | 1.027 | 2p15 | USP34 |
| RP11-7H17 | 1.008 | 18q23 | ATP9B. NFATC1 |
| RP11-53C3 | 1.000 | 12p12.1 | SSPN |

experiments were tested using normal versus normal hybridizations, which were performed simultaneously with the xenograft sample hybridization. On the basis of the control experiments, we used $log_2$ratio threshold of more than 0.25 for DNA copy number gains and $log_2$ratio less than – 0.25 for DNA copy number losses. High level copy number alterations (defined as $log_2$ratio more than 1) were seen on 34 (Table 2), including the LETM2, FGFR1 (8p12-8p11.23), C-MYC (8q24.21), CCND1 (11q13.2-11q13.3), ErbB2 (17q12) oncogenes, whereas homozygous deletions (defined as $log_2$ratio less than or equal to 1) were observed on 52 clones Table 3. Most of these deletions were seen on 8p21-8p23 (26 clones), on 14q31.11-14q32.14 (11 clones) and on 15q21.1-15q21.3 (6 clones). Figure 2 shows the whole genome aCGH profile of the B585 genome. High level amplification exceeding $log_2$ mean raw ratio more than 2 was present only in a few clones. In order to validate the copy number alterations observed by array CGH interphase FISH was applied using different combination of centromeric and locus specific probes.

### 4.3. Fluorescence *in situ* hybridization using centromere and gene specific probes

The ploidy pattern of the B585 cells were determined using 13 different centromere specific probes (chromosomes 1, 2, 5- 9, 11, 12, 17, 18, 20 and X). Chromosome index (CI: total number of centromeric signals/number of nuclei counted), which is closely related to the DNA content of the tumor, was calculated as 3.35 (Table 4). High level amplification was detected for the C-MYC (8q24.21), CCND1 (11q13.2-11q13.3), ErbB2, TOP2A (17q12) and intermediate amplification for the EGFR (7p12) and EGR1 (5q34) oncogenes. Interestingly only one or two copies (in relation to the chromosome 2 centromere) were deleted of the N-MYC (2p23-24) oncogene in the majority of cells. The deletion was also seen by aCGH. Summary of the FISH and aCGH data are presented for the studied regions in Table 5.

Chromosome 8 copy number alterations were greatly complex. High level amplification was seen on the 8p11.2 (clones: RP11-48D21, RP11-282J24, RP11-73M19) covering the FGFR-1 gene (Fibroblast growth factor receptor-1 gene) and on 8q24.1, 8q24.12-q13 and 8q24.2 which harbor the C-MYC oncogene. Deletion of the proximal part of the short arm (8p12-pter) was observed (Figure 3A). To validate the deletions at the 8p12 region and the amplification at the 8q24 loci we performed FISH

**Table 3.** Homozygoues deletions in the B585 genome detected by array CGH

| Clone | Log2Rat | Cromosome band | Genes covered by the clone | Gene name |
|---|---|---|---|---|
| RP11-82K8 | -1,533027 | 8p23.3 | MYOM2 | myomesin 2 |
| RP11-236O1 | -1,486447 | 8p22 | TUSC3 | tumor suppressor candidate 3 |
| CTD-2015D3 | -1,435987 | 8p21.2 | ADRA1A | alpha-1a-adrenergic receptor |
| RP11-51C1 | -1,31948 | 8p21.3 | ChGn | |
| RP11-76B12 | -1,311081 | 8p21.2 | DOCK5 | |
| RP11-140K14 | -1,280833 | 8p23.2 | CSMD1 | cub and sushi multiple domains 1 |
| RP11-164H24 | -1,269827 | 8p21.2 | KCTD9, PPP2R2A | protein phosphatase 2, regulatory subunit b, alpha |
| RP11-107P5 | -1,250866 | 8p22 | SLC7A2 | solute carrier family 7 (cationic amino acid transporter, y+ system), member 2 |
| RP11-252K12 | -1,245451 | 8p23.1 | XKR6 | |
| RP11-92C1 | -1,226788 | 8p22 | DLC1 | deleted in liver cancer 1 |
| RP11-241I4 | -1,209207 | 8p23.1 | MSRA | peptide methionine sulfoxide reductase |
| CTD-2105I3 | -1,200758 | 8p22 | PDGFRL | platelet-derived growth factor receptor-like |
| RP11-122D17 | -1,198927 | 8p12 | NRG1 | neuregulin 1 |
| RP11-158F9 | -1,19686 | 8p21.2 | | |
| RP11-233H21 | -1,147496 | 8p21.3 | INTS10 | integrator complex subunit 10 |
| GS1-77L23 | -1,138796 | 8 p tel | | |
| RP11-232J22 | -1,131851 | 8p21.2 | BNIP3L | bcl2/adenovirus e1b 19-kd protein-interacting protein 3-like |
| RP11-235F10 | -1,117739 | 8p23.1 | | |
| RP11-110I16 | -1,115802 | 8p21.3 | | |
| RP11-57I3 | -1,090498 | 8p12 | NRG1 | neuregulin 1 |
| RP11-112G9 | -1,076076 | 8p23.1 | MSRA | peptide methionine sulfoxide reductase |
| RP11-204M16 | -1,070723 | 8p21.3 | LOXL2, ENTPD4, | lysyl oxidase-like 2 |
| RP11-274F14 | -1,070167 | 8p12 | UNC5D | |
| RP11-274K12 | -1,051544 | 8p22 | | |
| RP11-262B7 | -1,036765 | 8p23.1 | CTSB | cathepsin b |
| RP11-235I5 | -1,033408 | 8p23.1 | GATA4, NEIL2, FDFT1, | gata-binding protein 4, endonuclease viii-like 2, farnesyldiphosphate farnesyltransferase 1 |
| RP11-274M9 | -1,031048 | 8p21.2 | PEBP4 | |
| RP11-182G2 | -1,004599 | 8p22 | TUSC3 | tumor suppressor candidate 3 |
| RP11-94C16 | -1,070268 | 11q23.2-11q23.3 | TRIM29 | tripartite motif-containing protein 29 |
| RP11-82I16 | -1,296506 | 12q22 | MRPL42 | |
| RP11-160P21 | -1,434434 | 14q32.13 | KIAA1622 | |
| RP11-28G16 | -1,255502 | 14q32.12 | SLC24A4 | solute carrier family 24 (sodium/potassium/calcium exchanger), member 4 |
| RP11-121H7 | -1,194264 | 14q32.31 | PPP2R5C | |
| RP11-40P23 | -1,192330 | 14q31.3-14q32.11 | CHES1 | checkpoint suppressor 1 |
| RP11-111F22 | -1,134278 | 14q32.2 | CCNK | cyclin k |
| RP11-188G21 | -1,131224 | 14q32.12 | LGMN | |
| RP11-26J5 | -1,088568 | 14q32.13 | KIAA1622, SERPINA10, SERPINA6, SERPINA1 | protein z-dependent protease inhibitor precursor |
| RP11-30I7 | -1,200377 | 15q21.3 | RFXDC2 | |
| RP11-221H24 | -1,139980 | 15q21.1 | ONECUT1 | one cut homeobox 1 |
| RP11-61K4 | -1,091610 | 15q21.3 | PRTG | |
| RP11-25G4 | -1,063665 | 15q21.3 | PRTG | |
| CTB-305D20 | -1,622018 | 17q21.32 | WNT3 | wingless-type mmtv integration site family, member 3 |

**Table 4.** Copy number distribution of centromeric probes in B585 interphase cells by FISH

| **Chromosomes** | | | | | | | | | | | | | |
|---|---|---|---|---|---|---|---|---|---|---|---|---|---|
| **Signals/ cells** | **1** | **2** | **5** | **6** | **7** | **8** | **9** | **11** | **12** | **17** | **18** | **20** | **X** |
| **0** | 0 | 2 | 3 | 0.7 | 0 | 0 | 0 | 0 | 0.8 | 0 | 0 | 0 | 0 |
| **Less than or equals to 1** | 0 | 2 | 2 | 0.7 | 0 | 0 | 0 | 0 | 0.8 | 0 | 0 | 0 | 0 |
| **2** | 0 | 2 | 0 | 17 | 0.7 | 6 | 8.2 | 0.5 | 7.1 | 20.7 | 4.2 | 7.3 | ***25.1*** |
| **3** | 12.2 | ***42***[1] | ***75*** | ***68*** | 21.2 | ***43*** | ***43.2*** | ***80*** | ***70.1*** | ***67.9*** | ***29.8*** | ***27.8*** | ***57*** |
| **4** | ***36.7*** | ***41*** | 4 | 5.4 | ***65*** | ***41*** | ***42.1*** | 4 | 1.6 | 5.4 | ***55.8*** | ***52.3*** | 3 |
| **5** | ***36.2*** | 3.5 | 7 | 1.4 | 4 | 1.5 | 1.1 | 14 | 11.8 | 3 | 1.4 | 7.3 | 4 |
| **More than or equals to 6** | 14.1 | 9.5 | 9 | 7.5 | 9.1 | 7.5 | 5.4 | 1.5 | 8.6 | 3 | 8.8 | 5.3 | 10.9 |
| **Number of cells analysed** | 376 | 200 | 167 | 147 | 151 | 201 | 183 | 214 | 127 | 368 | 215 | 151 | 175 |

[1] dominant cell populations are labeled with bold italic

analysis at a single cell level using tricolor FISH, containing the CEP® 8 probe labeled with SpectrumAqua, lipoprotein lipase (LPL) labeled with SpectrumOrange and the C-MYC gene labeled with SpectrumGreen (Figure 3C). A separate experiment was performed using the 8p22 probe simultaneously with chromosome 8 centromere. The interphase FISH results are summarized on Figure 3B. Chromosome 8 centromere were present mainly in three copies (66%), whereas the 8p22 locus was deleted in more than 75% of cells, the C-MYC oncogene was amplified in 55% of cells (amplification level is approximately 4 fold relative to the centromeric 8 signals) and the 8p22 locus was deleted in more 65% of cells.

Out of the 192 BAC clones covering chromosome 11 nineteen were amplified at the 11q13-q14

**Table 5.** Comparison of FISH and array CGH data of B585 cells

| | Gene localization | Definition of gene alteration based on FISH data (range of number of copies/ signals/cell) | $Log_2$ ratio by array CGH | Major population based on centromere counts |
|---|---|---|---|---|
| Chr 2 N-MYC | 2p23-24 | deletion (1-2) | -0.39534 | trisomic |
| Chr 5 EGR 1 | 5q34 | intermediate amplification (3-10) | +0.32963 | trisomic |
| Chr 7 EGFR | 7p12 | intermediate amplification (3-10) | +0.31331 | trisomic |
| Chr8 C-MYC | 8q24 | high level amplification (more than 20) | +2.11409 | heterogeneous trisomic/tetrasomic |
| Chr 11 CCND1 | 11q13 | high level amplification (more than 20) | +1.12712 | Heterogeneous trisomic/tetrasomic |
| Chr 17 ErBB2 TOPO2 | **Chr 17** 17q11.3 17q21-22 | ERbB2 and the TOPO2 genes are coamplified and the signal distribution is heterogeneous (5-30) | **Chr 17** +1.24382 +0.00812 | trisomic |

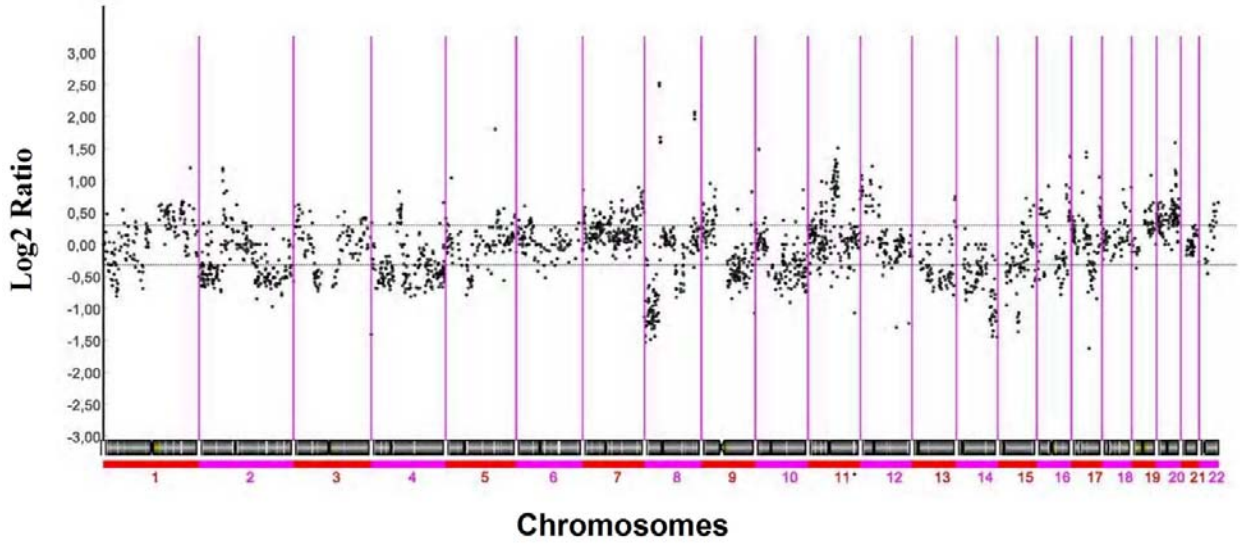


**Figure 2.** Array CGH profile of the B585 xenograft. B585 and female reference DNAs were labeled and hybridized to HumArray 3.2 BAC microarray comprised of 2.464-clones representing all chromosomes. Clones are ordered from chromosome 1-22 and within each chromosome on the basis of UCSC mapping position (http://genome.ucsc.edu). Threshold for copy number gains and losses are shown in dashed line (gains +0.25 and losses – 0.25).

region. By using FISH we could detect high copy number amplification of the CCND1 gene. The amplification pattern of CCDN1 was heterogeneous; there was a significant fraction of cells having more than 20 signals.

Figure 4A shows the aCGH profile of chromosome 17 of the B585 xenograft. Two regions were amplified on chromosome 17, one is the ErbB2 (17q12) and the second is 17q24-25 loci containing the MAP2K6 (mitogen-activated protein kinase kinase 6: 17q24.3) and the GRB2 (growth factor receptor-bound protein 2: 17q24-25) genes. Using chromosomal CGH we could not detect gain on 17q12 (Table 1.), however array CGH showed clear amplification of this loci. The amplification of the 17q12 was validated by FISH with three color probe set (LSI® TOP2A SpectrumOrange™ /HER-2 SpectrumGreen™ CEP® 17 SpectrumAqua™), Figure 4B illustrates the distribution of these genes and the Figure 4C demonstrates a representative FISH image clearly showing the coamplification of ErbB2 and TOP2A on the magnified image part: green fluorescent spots (ERbB2 signals) are frequently very close to the red spots (TOP2A).

### 4.4. Gene expression signature of the B585 xenograft

Gene expression signature of the B585 cells were defined on Affymetrix GeneChip Human Genome U133 Plus 2.0 expression arrays. After the normalization and quality control steps Volcano plot p-value cutoff 0.05 with Benjamini and Hochberg False Discovery Rate was applied to identify genes differentially expressed (more than 2 – fold) between the B585 cells and control sample. Affymetrix gene expression analysis resulted in 564 differentially expressed genes, raging from 145-fold increased in odontogenic ameloblast-associated protein to an 82.8-fold decrease in SPARC-like 1. Out of these genes 416 were found to be upregulated and 148 downregulated in B585 cells versus normal breast sample. Overexpression of different genes was detected on all chromosomes. Correlation of gene expression level and gene amplification was also performed. Out of the 44 amplified genes we could identify 37 different transcripts on the

**Table 6.** Correlation of gene amplification and gene expression in B585 cells

| BAC Clone ID | Chromosome localisation | aCGH Log2 Ratio | Representative genes | Affymetrix ID | Fold change |
|---|---|---|---|---|---|
| **RP1-88B16** | **11q13.2-q13.3** | **1.01** | **CCND1** | **208711_s_at** | **3.97** |
| RP1-17L4 | 11q13.2-q13.3 | 1.07 | FGF4 | 206783_at | 1.23 |
| RP11-7H17 | 18q23 | 1.01 | ATP9B | 214934_at | 1.71 |
| | | | **NFATC1** | **210162_s_at** | **7.04** |
| RP11-102M18 | 11q13.4 | 0.98 | UCP2,UPC3 | 208998_at | 1.55 |
| | | | WDR71 | 218957_s_at | 1.95 |
| | | | DKFZP586P0123 | 36552_at | 2.84 |
| RP11-53C3 | 12p12.1 | 0.99 | SSPN | 204963_at | -2.64 |
| **RP11-64N21** | **12p11.23** | **1.01** | **STK38L** | **212565_at** | **7.50** |
| CTC-298G6 | 12p13.32 | 1.02 | CCND2 | 200953_s_at | -8.76 |
| **RP11-675B4** | **11q13.1** | **1.05** | **SF3B2** | **200619_at** | **3.15** |
| RP11-24P23 | 2p14-p13.3 | 1.08 | TGFA | 205016_at | 2.48 |
| **RP11-24N12** | **12p13.33-p13.32** | **1.08** | **TEAD4** | **41037_at** | **6.95** |
| CTD-2125H12 | 20q13.3 | 1.12 | CEBPB | 212501_at | 2.40 |
| RP11-17D23 | 2p15 | 1.15 | USP34 | 212066_s_at | 2.83 |
| RP11-149G19 | 11q13.2 | 1.16 | LRP5 | 209468_at | 2.09 |
| RP11-192M1 | 1q42.12 | 1.20 | TMEM63A | 214833_at | 2.23 |
| | | | PYCR2 | 224855_at | 3.18 |
| CTD-2018D13 | 2p14-p13.3 | 1.21 | TGFA | 205016_at | 2.48 |
| RP11-120P20 | 11q13.3 | 1.22 | SHANK2 | 213308_at | 3.47 |
| RP11-78F16 | 12p11.21 | 1.22 | EEG-1 | 218456_at | 2.49 |
| RP11-168B13 | 11q13.4-q13.5 | 1.27 | RPS3 | 200019_s_at | 1.77 |
| | | | GDPD5 | 32502_at | 3.75 |
| CTC-437H15 | 11q13.3 | 1.33 | CTTN | 213308_at | 3.47 |
| **DMPC-HFF#1-61H8** | **17q12** | **1.36** | **ERBB2** | **216836_s_at** | **8.27** |
| RP11-122P17 | 16q24.1 | 1.37 | IRF-8 | 204057_at | -2.01 |
| RP11-118F19 | 16q24.1 | 1.38 | KIAA0182 | 212056_at | 3.00 |
| | | | **GINS2** | **221521_s_at** | **15.07** |
| **DMPC-HFF#1-61H8** | **17q12** | **1.44** | **ERBB2** | **216836_s_at** | **8.27** |
| **GS-7N12** | **11q13.5-q14.1** | **1.51** | **PAK1** | **230100_at** | **5.41** |
| RP11-282J24 | 8p11.21 | 1.61 | ANK1 | 240363_at | 1.25 |
| RP11-237F24 | 8q24.21 | 2.03 | MYC | 202431_s_at | 1.92 |
| RP11-265K5 | 8p12 | 2.48 | LETM2 | 1557415_s_at | 1.34 |
| | | | FGFR1 | 215404_x_at | 2.13 |
| | | | **WHSC1L1** | **218173_s_at** | **4.23** |
| | | | **PPAPDC1B** | **223568_s_at** | **6.19** |

Affymetrix Human 2 array (Table 6). From these thirty-seven genes we found only three (clone ID CTC-298G6 on 12p12.1, RP11-53C3 on 12p13.32 and RP11-122P17 on 16q24.1 regions) that were down regulated when compared to normal breast tissue expression level. The larger fraction (65%) of the amplified genes was overexpressed more than 2 - fold. The highest fold change was detected for the GINS2 (16q24.1) and ErbB2 genes. Relatively high fold change was noticed on genes that were amplified around the CCDN1 gene on chromosome 11q13.2-q13.3. Near this region, the expression level of the amplified PAK1 serine/threonine kinase was also increased. The mRNA level of the C-MYC genes was less prominent when compared to the normal sample, the fold change for this gene was less than 2. When we compared the expression level of genes that were selected based on their association with trastuzumab treatment response in human breast tumors, we found that the CCNE1, CDK1 and ErbB2 genes have the highest expression level (exceeding more than 8 fold over mean gene expression of the controls), other genes including the SKP2, FLNA, ITGB4, PRKDC, ERbB3, COP1, RELA, GRB7, RARA and FADD genes were also highly upregulated. Tumorsuppressor genes including PTEN, JAK1, MAPK1, TP53 ESR1, LYN, JUN and CAV2 genes were found to be downregulated in the B585 xenograft.

## 5. DISCUSSION

We report here the cytogenetic and immunohistochemical characterization of a human breast cancer cell line (B585) that was established from an invasive ductal breast carcinoma of a 63 year-old patient who was resistant to trastuzumab treatment (40). The B585 cells can grow only in immunodeficient mice, and the B585 xenografts are resistant to trastuzumab treatment similarly to the primary tumor (40).

Using chromosomal CGH we could compare the copy number alterations of the original tumor and the xenograft and found that most of the alterations were similar, which is a sign for the common clonal origin of lesions. This observation indicates that the cell line retained most of the genetic characteristics of the parental tumor. The divergence between the two samples can be explained in different ways: i.) the genetic make up of tumor cells in the xenograft are heterogeneous, but the ratio of cells exhibiting the different alterations is higher in the B585 xenograft than it was in the primary lesion, ii.) the normal cell contamination of the primary breast cancer tissue could mask some alterations present in a small fraction of cells, thus it may cover less dominant changes in a genetically heterogeneous tumor, in addition those cells can have higher proliferative rate in the xenograft, iii.) it can not be

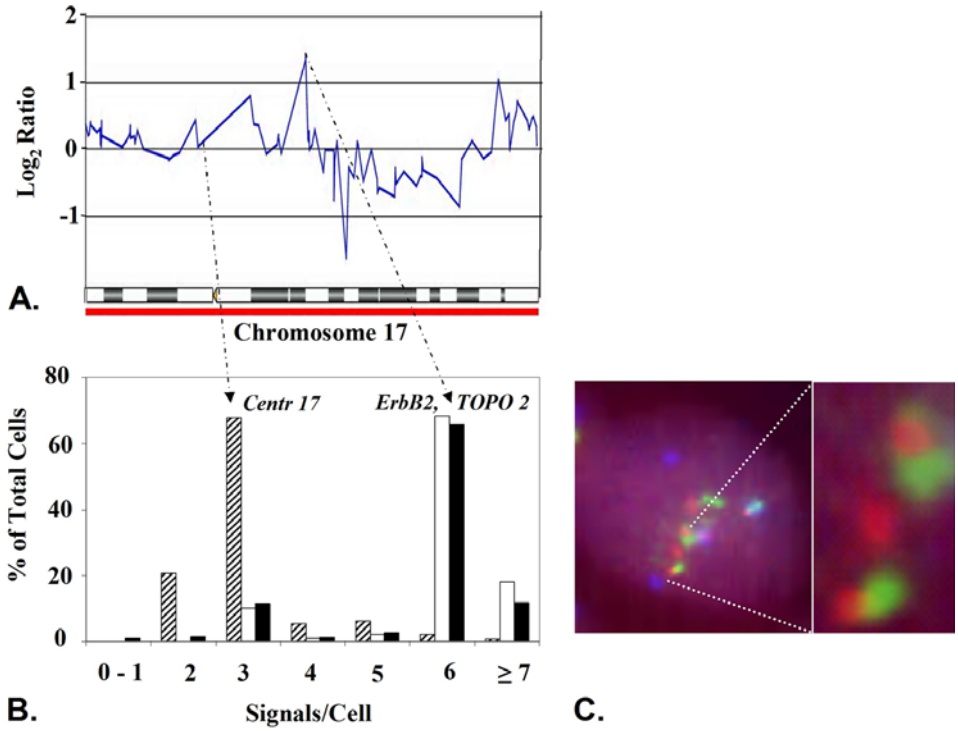


**Figure 3.** Validation of amplifications and deletions on chromosome 8 by FISH in interphase B585 cells. A.) array CGH profile of chromosome 8. B.) Distribution of centromere 8 (empty column), 8p22 (parquet column), 8q21.23 (hatched column) and 8q24.21 (black column) loci in the interphase cells of B585 xenograft. C.) Interphase FISH shows multiple signals for chromosome 8 centromere (blue spots), 8q21.23 region expresses two and one signals (red spots), the 8q24.21 region exhibit high level amplification (green spots).

excluded either that alterations seen only in the cell line are the results of *in vivo* cell culturing.

Because the resolution of cCGH is limited, to more precisely describe and map the chromosome copy number alterations we also performed array CGH analysis on B585 cells. The results of cCGH and aCGH analyses were highly concordant for the main regions identified by cCGH, however numerous single copy amplicons and small deletions, that were not seen by cCGH were also discovered by aCGH. High level of copy number alterations that are predictive for poor prognosis of breast cancer patients were all present in the B585 xenograft, those included amplifications on chromosome 8, 17 and 20 (51). The cytogenetic alterations detected by array CGH in the B585 genome are similar to the JIMT1 cell line, a recently described trastuzumab resistant cell line (51). Complex pattern of genomic alterations were detected in B585 on chromosomes 2, 4, 8 as well as chromosome 11q13, 16q and 17q. The highest level of amplification was seen on the 8p12-8p11.23 region which covers many genes including the FGFR1 (fibroblast growth factor receptor-1 (fms-related tyrosine kinase-2)) putative oncogene. It was found by others that chromosome 8p12-8p11.23 locus is amplified in 10-15% of human breast cancers (52). Amplification of this region has been associated with estrogen receptor-positive tumors and lobular histology (53). The FGFR1 is excluded from the amplicon in some tumors (54). There is less information available about the role of highly expressed genes on this locus, including LETM2, DDHD2, WHSC1L1 and PPAPDC1B which were overexpressed in B585 between 4 to 9 fold when compared to the expression values to normal breast tissue. Relatively high level amplification of the C-MYC was detected by aCGH which was also confirmed by FISH, the C-MYC and chromosome 8 ratio was 4 in more than 50% of cells and was above 6 in 12% of B585 cells. It has been shown that the C-MYC amplification was significantly associated with high histological grade, negative progesterone receptor status DNA aneuploidy, high S-phase fraction and with poor distant metastasis-free survival (55). However, we have to note that the amplification of the C-MYC oncogene in the B585 cell line was not associated with high mRNA level.

Chromosome locus 11q13 is frequently amplified in a number of human cancers including carcinoma of the breast (56, 57). Originally 11q13 amplification was thought to involve only a single amplicon spanning many megabases, but more recent data have identified four core regions within 11q13 that can be amplified independently or together in different combinations. The present CGH array data support this observation. The clustered amplifications on chromosome 11q13-14 region pin point that numerous genes are amplified around the CCND1 gene. This region harbors several genes with known or

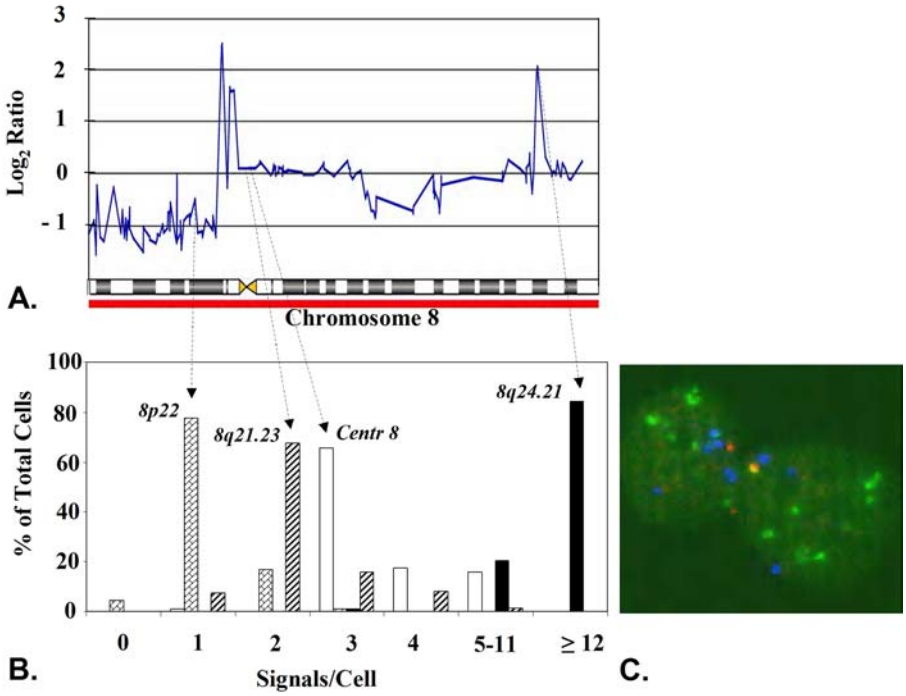


**Figure 4.** A.) Array CGH result of chromosome 17 of B585 cells. B.) Distribution of the ErbB2 (black column), TOP2A (empty column) and the centromeric 17 (hatched column) signals in interphase B585 cells. C.) ErbB2 (green signals) and TOP2A (red signals) genes exhibit CLEAR co-amplification in B585 xenograft cells. Chromosome 17 centromeric signal appears as blue spots in the cell nuclei.

suspected oncogenic potential, the complex structure of the amplicons and the fact that 11q13 is gene-rich locus have contributed to the identification of specific genes that contribute breast cancer tumorigenesis and make it a difficult and continuing process. To date CCND1 (encoding the cell cycle regulatory cyclin D1) and EMS1 (encoding the filamentous actin binding protein and c-Src substrate cortactin) are the favored candidates (58).

Several reports have documented that close to the nearby TOP2A gene is often coamplified or deleted in breast carcinomas with ErbB2 amplification, and recent finding suggests that coamplification plays an important role in facilitating a favorable response to antracyclines, which target topoisomerase IIa (59). Another report has shown that several genes between ErbB2 and TOP2-A are often coexpressed in breast carcinoma cell lines with amplification of the ErbB2 gene. This opens the possibility that these other genes may play an important role in determining malignant potential and response to therapy, including trastuzumab.

Affymetrix gene expression analysis showed differentially upregulated and downregulatred genes. The set of highly expressed genes includes many genes with functional roles in cell cycle regulation and proliferation such as CDKN2B, CDC23, MCM8 and RFC2 as well as genes that are involved in cytokine-cytokine receptor interactions such as the CCL19, VEGFA genes. Increased expression levels of TOP2A and ErbB2 genes were detected. While the expression levels of ErbB3 protein (the preferred and most potent dimerization partner of ErbB2 (60) and ErbB4 are low on B585 cells (our unpublished observations), the ligand-less ErbB2 may recruit ErbB1, (which is overexpressed in B585 cells, Figure 1F), to boost its signaling potential through ErbB1. Recently, the involvement of ErbB2 in non-ErbB protein-mediated signaling has been brought into the focus of cancer research. Among these, beta integrins and CD44 are probably the best known candidates whose roles in cancer progression are well documented (61-64). In addition, CD44 is also involved in the direct regulation of both ErbB2 and ErbB1 (63). Furthermore, while ADCC had a key role in the tumor inhibitory effect of trastuzumab *in vivo* (27, 65), and CD44 was also suggested being able to prevent the recruitment of Fc receptor bearing immune effector cells, the B585 model (we showed that both integrin beta 1 and CD44 are overexpressed on B585 cells) may provide a suitable system to investigate the role of integrin beta 1 and CD44 in the trastuzumab resistance, especially in the resistance against trastuzumab-mediated ADCC. Furthermore, we found that epithelial specific antigen (ESA), a cell surface molecule that is known to be highly expressed in primary and metastatic breast cancer (66, 67) and together with CD44 have also been identified as prospective marker for breast cancer stem cells (68, 69) are also overexpressed on B585 cells.

In summary we have described a detailed characterization of a recently established trastuzumab-resistant breast cancer xenograft, B585. The B585 cells exhibit chromosomal alterations that are characteristic for

breast tumors with a highly aggressive phenotype. The copy number alterations of the original primary tumor and the xenograft are similar. Beside known alterations numerous new copy number changes were identified. The B585 xenografts are resistant to trastuzumab administration, in spite of that the B585 cells are heterogeneously amplified for the ErbB2 gene and carry a high level mRNA and an intermediate protein expression for ErbB2, those histological features are representative for highly invasive trastuzumab-resistant ductal breast carcinoma that makes the B585 cells suitable model to study trastuzumab-resistance in model experiments and to use to assess potential therapies for this type of breast tumors.

## 6. AKNOWLEDGEMENT

Mark Barok and Margit Balazs contributed equally to this work. The study was supported by the following grants Hungarian Academy of Sciences (2006TKI247), Hungarian Scientific Research Fund, OTKA T 048750, T 75191, T 68763, K62648, 75752, University of Debrecen, Hungary Mecenatura 1620 29/0017/1/29, NIH P50 CA58207, FIRCA R03 TW 00871-01A2, EU FP6 LSHB-CT-2004-503467, LSHC-CT-2005-018914, MCRTN-CT-035946-2, and MRTN-CT-2005-019481.

## 7. REFERENCES

1. Park JW, RM Neve, J Szollosi, CC Benz: Unraveling the biologic and clinical complexities of HER2. *Clin Breast Cancer* 8, 392-401 (2008)

2. Friedlander E, M Barok, J Szollosi, G Vereb: ErbB-directed immunotherapy: antibodies in current practice and promising new agents. *Immunol Lett* 116, 126-140 (2008)

3. Bublil EM, Y Yarden: The EGF receptor family: spearheading a merger of signaling and therapeutics. *Curr Opin Cell Biol* 19, 124-134 (2007)

4. Landgraf R: HER2 therapy. HER2 (ERBB2): functional diversity from structurally conserved building blocks. *Breast Cancer Res* 9, 202 (2007)

5. Klapper LN, S Glathe, N Vaisman, NE Hynes, GC Andrews, M Sela, Y Yarden: The ErbB-2/HER2 oncoprotein of human carcinomas may function solely as a shared coreceptor for multiple stroma-derived growth factors. *Proc Natl Acad Sci U S A* 96, 4995-5000 (1999)

6. Klapper LN, MH Kirschbaum, M Sela, Y Yarden: Biochemical and clinical implications of the ErbB/HER signaling network of growth factor receptors. *Adv Cancer Res* 77, 25-79 (2000)

7. Pierce JH, P Arnstein, E DiMarco, J Artrip, MH Kraus, F Lonardo, PP Di Fiore, SA Aaronson: Oncogenic potential of erbB-2 in human mammary epithelial cells. *Oncogene* 6, 1189-1194 (1991)

8. Slamon DJ, W Godolphin, LA Jones, JA Holt, SG Wong, DE Keith, WJ Levin, SG Stuart, J Udove, A Ullrich, et al.: Studies of the HER-2/neu proto-oncogene in human breast and ovarian cancer. *Science* 244, 707-712 (1989)

9. Aigner A, H Juhl, C Malerczyk, A Tkybusch, CC Benz, F Czubayko: Expression of a truncated 100 kDa HER2 splice variant acts as an endogenous inhibitor of tumour cell proliferation. *Oncogene* 20, 2101-2111 (2001)

10. Andrechek ER, WR Hardy, PM Siegel, MA Rudnicki, RD Cardiff, WJ Muller: Amplification of the neu/erbB-2 oncogene in a mouse model of mammary tumorigenesis. *Proc Natl Acad Sci U S A* 97, 3444-3449 (2000)

11. Moody SE, CJ Sarkisian, KT Hahn, EJ Gunther, S Pickup, KD Dugan, N Innocent, RD Cardiff, MD Schnall, LA Chodosh: Conditional activation of Neu in the mammary epithelium of transgenic mice results in reversible pulmonary metastasis. *Cancer Cell* 2, 451-461 (2002)

12. Slamon DJ, B Leyland-Jones, S Shak, H Fuchs, V Paton, A Bajamonde, T Fleming, W Eiermann, J Wolter, M Pegram, J Baselga, L Norton: Use of chemotherapy plus a monoclonal antibody against HER2 for metastatic breast cancer that overexpresses HER2. *N Engl J Med* 344, 783-792 (2001)

13. Cobleigh MA, CL Vogel, D Tripathy, NJ Robert, S Scholl, L Fehrenbacher, JM Wolter, V Paton, S Shak, G Lieberman, DJ Slamon: Multinational study of the efficacy and safety of humanized anti-HER2 monoclonal antibody in women who have HER2-overexpressing metastatic breast cancer that has progressed after chemotherapy for metastatic disease. *J Clin Oncol* 17, 2639-2648 (1999)

14. Burstein HJ, I Kuter, SM Campos, RS Gelman, L Tribou, LM Parker, J Manola, J Younger, U Matulonis, CA Bunnell, AH Partridge, PG Richardson, K Clarke, LN Shulman, EP Winer: Clinical activity of trastuzumab and vinorelbine in women with HER2-overexpressing metastatic breast cancer. *J Clin Oncol* 19, 2722-2730 (2001)

15. Pegram MD, A Lipton, DF Hayes, BL Weber, JM Baselga, D Tripathy, D Baly, SA Baughman, T Twaddell, JA Glaspy, DJ Slamon: Phase II study of receptor-enhanced chemosensitivity using recombinant humanized anti-p185HER2/neu monoclonal antibody plus cisplatin in patients with HER2/neu-overexpressing metastatic breast cancer refractory to chemotherapy treatment. *J Clin Oncol* 16, 2659-2671 (1998)

16. Cardoso F, MJ Piccart, V Durbecq, A Di Leo: Resistance to trastuzumab: a necessary evil or a temporary challenge? *Clin Breast Cancer* 3, 247-257; discussion 258-249 (2002)

17. Tanner M, P Jarvinen, J Isola: Amplification of HER-2/neu and topoisomerase IIalpha in primary and metastatic breast cancer. *Cancer Res* 61, 5345-5348 (2001)

18. Hudziak RM, GD Lewis, M Winget, BM Fendly, HM Shepard, A Ullrich: p185HER2 monoclonal antibody has antiproliferative effects in vitro and sensitizes human breast tumor cells to tumor necrosis factor. *Mol Cell Biol* 9, 1165-1172 (1989)

19. Yakes FM, W Chinratanalab, CA Ritter, W King, S Seelig, CL Arteaga: Herceptin-induced inhibition of phosphatidylinositol-3 kinase and Akt Is required for antibody-mediated effects on p27, cyclin D1, and antitumor action. *Cancer Res* 62, 4132-4141 (2002)

20. Lane HA, AB Motoyama, I Beuvink, NE Hynes: Modulation of p27/Cdk2 complex formation through 4D5-mediated inhibition of HER2 receptor signaling. *Ann Oncol* 12, S21-22 (2001)

21. Nagy P, A Jenei, S Damjanovich, TM Jovin, J Szolosi: Complexity of signal transduction mediated by ErbB2: clues to the potential of receptor-targeted cancer therapy. *Pathol Oncol Res* 5, 255-271 (1999)

22. Sliwkowski MX, JA Lofgren, GD Lewis, TE Hotaling, BM Fendly, JA Fox: Nonclinical studies addressing the mechanism of action of trastuzumab (Herceptin). *Semin Oncol* 26, 60-70 (1999)

23. Cuello M, SA Ettenberg, AS Clark, MM Keane, RH Posner, MM Nau, PA Dennis, S Lipkowitz: Down-regulation of the erbB-2 receptor by trastuzumab (herceptin) enhances tumor necrosis factor-related apoptosis-inducing ligand-mediated apoptosis in breast and ovarian cancer cell lines that overexpress erbB-2. *Cancer Res* 61, 4892-4900 (2001)

24. Nagata Y, KH Lan, X Zhou, M Tan, FJ Esteva, AA Sahin, KS Klos, P Li, BP Monia, NT Nguyen, GN Hortobagyi, MC Hung, D Yu: PTEN activation contributes to tumor inhibition by trastuzumab, and loss of PTEN predicts trastuzumab resistance in patients. *Cancer Cell* 6, 117-127 (2004)

25. Kono K, E Sato, H Naganuma, A Takahashi, K Mimura, H Nukui, H Fujii: Trastuzumab (Herceptin) enhances class I-restricted antigen presentation recognized by HER-2/neu-specific T cytotoxic lymphocytes. *Clin Cancer Res* 10, 2538-2544 (2004)

26. Izumi Y, L Xu, E di Tomaso, D Fukumura, RK Jain: Tumour biology: herceptin acts as an anti-angiogenic cocktail. *Nature* 416, 279-280 (2002)

27. Barok M, J Isola, Z Palyi-Krekk, P Nagy, I Juhasz, G Vereb, P Kauraniemi, A Kapanen, M Tanner, J Szollosi: Trastuzumab causes antibody-dependent cellular cytotoxicity-mediated growth inhibition of submacroscopic JIMT-1 breast cancer xenografts despite intrinsic drug resistance. *Mol Cancer Ther* 6, 2065-2072 (2007)

28. Clynes RA, TL Towers, LG Presta, JV Ravetch: Inhibitory Fc receptors modulate in vivo cytoxicity against tumor targets. *Nat Med* 6, 443-446 (2000)

29. Motoyama AB, NE Hynes, HA Lane: The efficacy of ErbB receptor-targeted anticancer therapeutics is influenced by the availability of epidermal growth factor-related peptides. *Cancer Res* 62, 3151-3158 (2002)

30. Lu Y, X Zi, M Pollak: Molecular mechanisms underlying IGF-I-induced attenuation of the growth-inhibitory activity of trastuzumab (Herceptin) on SKBR3 breast cancer cells. *Int J Cancer* 108, 334-341 (2004)

31. Price-Schiavi SA, S Jepson, P Li, M Arango, PS Rudland, L Yee, KL Carraway: Rat Muc4 (sialomucin complex) reduces binding of anti-ErbB2 antibodies to tumor cell surfaces, a potential mechanism for herceptin resistance. *Int J Cancer* 99, 783-791 (2002)

32. Nagy P, E Friedlander, M Tanner, AI Kapanen, KL Carraway, J Isola, TM Jovin: Decreased accessibility and lack of activation of ErbB2 in JIMT-1, a herceptin-resistant, MUC4-expressing breast cancer cell line. *Cancer Res* 65, 473-482 (2005)

33. Pályi-Krekk Z, M Barok, J Isola, M Tammi, J Szöllősi, P Nagy: Hyaluronan-induced masking of ErbB2 and CD44-enhanced trastuzumab internalization in trastuzumab resistant breast cancer *European Journal Of Cancer* (2007)

34. Kono K, A Takahashi, F Ichihara, H Sugai, H Fujii, Y Matsumoto: Impaired antibody-dependent cellular cytotoxicity mediated by herceptin in patients with gastric cancer. *Cancer Res* 62, 5813-5817 (2002)

35. Mimura K, K Kono, M Hanawa, M Kanzaki, A Nakao, A Ooi, H Fujii: Trastuzumab-mediated antibody-dependent cellular cytotoxicity against esophageal squamous cell carcinoma. *Clin Cancer Res* 11, 4898-4904 (2005)

36. Kute T, CM Lack, M Willingham, B Bishwokama, H Williams, K Barrett, T Mitchell, JP Vaughn: Development of Herceptin resistance in breast cancer cells. *Cytometry A* 57, 86-93 (2004)

37. Ritter CA, M Perez-Torres, C Rinehart, M Guix, T Dugger, JA Engelman, CL Arteaga: Human Breast Cancer Cells Selected for Resistance to Trastuzumab In vivo Overexpress Epidermal Growth Factor Receptor and ErbB Ligands and Remain Dependent on the ErbB Receptor Network. *Clin Cancer Res* 13, 4909-4919 (2007)

38. Tanner M, AI Kapanen, T Junttila, O Raheem, S Grenman, J Elo, K Elenius, J Isola: Characterization of a novel cell line established from a patient with Herceptin-resistant breast cancer. *Mol Cancer Ther* 3, 1585-1592 (2004)

39. Rennstam K, G Jonsson, M Tanner, PO Bendahl, J Staaf, AI Kapanen, R Karhu, B Baldetorp, A Borg, J Isola: Cytogenetic characterization and gene expression profiling of the trastuzumab-resistant breast cancer cell

line JIMT-1. *Cancer Genet Cytogenet* 172, 95-106 (2007)

40. Marx C, C Berger, F Xu, C Amend, GK Scott, B Hann, JW Park, CC Benz: Validated high-throughput screening of drug-like small molecules for inhibitors of ErbB2 transcription. *Assay Drug Dev Technol* 4, 273-284 (2006)

41. Bosma GC, M Fried, RP Custer, A Carroll, DM Gibson, MJ Bosma: Evidence of functional lymphocytes in some (leaky) scid mice. *J Exp Med* 167, 1016-1033 (1988)

42. Balazs M, Z Adam, A Treszl, A Begany, J Hunyadi, R Adany: Chromosomal imbalances in primary and metastatic melanomas revealed by comparative genomic hybridization. *Cytometry* 46, 222-232 (2001)

43. Treszl A, A Ladanyi, Z Rakosy, Z Buczko, R Adany, M Balazs: Molecular cytogenetic characterization of a novel cell line established from a superficial spreading melanoma. *Front Biosci* 11, 1844-1853 (2006)

44. Snijders AM, N Nowak, R Segraves, S Blackwood, N Brown, J Conroy, G Hamilton, AK Hindle, B Huey, K Kimura, S Law, K Myambo, J Palmer, B Ylstra, JP Yue, JW Gray, AN Jain, D Pinkel, DG Albertson: Assembly of microarrays for genome-wide measurement of DNA copy number. *Nat Genet* 29, 263-264 (2001)

45. Pinkel D, R Segraves, D Sudar, S Clark, I Poole, D Kowbel, C Collins, WL Kuo, C Chen, Y Zhai, SH Dairkee, BM Ljung, JW Gray, DG Albertson: High resolution analysis of DNA copy number variation using comparative genomic hybridization to microarrays. *Nat Genet* 20, 207-211 (1998)

46. Jain AN, TA Tokuyasu, AM Snijders, R Segraves, DG Albertson, D Pinkel: Fully automatic quantification of microarray image data. *Genome Res* 12, 325-332 (2002)

47. Bussey KJ, D Kane, M Sunshine, S Narasimhan, S Nishizuka, WC Reinhold, B Zeeberg, W Ajay, JN Weinstein: MatchMiner: a tool for batch navigation among gene and gene product identifiers. *Genome Biol* 4, R27 (2003)

48. Rakosy Z, L Vizkeleti, S Ecsedi, Z Voko, A Begany, M Barok, Z Krekk, M Gallai, Z Szentirmay, R Adany, M Balazs: EGFR gene copy number alterations in primary cutaneous malignant melanomas are associated with poor prognosis. *Int J Cancer* 121, 1729-1737 (2007)

49. Juhasz A, M Balazs, I Sziklay, Z Rakosy, A Treszl, G Repassy, R Adany: Chromosomal imbalances in laryngeal and hypopharyngeal cancers detected by comparative genomic hybridization. *Cytometry A* 67, 151-160 (2005)

50. Szollosi J, M Balazs, BG Feuerstein, CC Benz, FM Waldman: ERBB-2 (HER2/neu) gene copy number, p185HER-2 overexpression, and intratumor heterogeneity in human breast cancer. *Cancer Res* 55, 5400-5407 (1995)

51. Rennstam K, M Ahlstedt-Soini, B Baldetorp, PO Bendahl, A Borg, R Karhu, M Tanner, M Tirkkonen, J Isola: Patterns of chromosomal imbalances defines subgroups of breast cancer with distinct clinical features and prognosis. A study of 305 tumors by comparative genomic hybridization. *Cancer Res* 63, 8861-8868 (2003)

52. Ray ME, ZQ Yang, D Albertson, CG Kleer, JG Washburn, JA Macoska, SP Ethier: Genomic and expression analysis of the 8p11-12 amplicon in human breast cancer cell lines. *Cancer Res* 64, 40-47 (2004)

53. Courjal F, M Cuny, J Simony-Lafontaine, G Louason, P Speiser, R Zeillinger, C Rodriguez, C Theillet: Mapping of DNA amplifications at 15 chromosomal localizations in 1875 breast tumors: definition of phenotypic groups. *Cancer Res* 57, 4360-4367 (1997)

54. Dib A, J Adelaide, M Chaffanet, A Imbert, D Le Paslier, J Jacquemier, P Gaudray, C Theillet, D Birnbaum, MJ Pebusque: Characterization of the region of the short arm of chromosome 8 amplified in breast carcinoma. *Oncogene* 10, 995-1001 (1995)

55. Rummukainen JK, T Salminen, J Lundin, H Joensuu, JJ Isola: Amplification of c-myc oncogene by chromogenic and fluorescence in situ hybridization in archival breast cancer tissue array samples. *Lab Invest* 81, 1545-1551 (2001)

56. Clark ES, B Brown, AS Whigham, A Kochaishvili, WG Yarbrough, AM Weaver: Aggressiveness of HNSCC tumors depends on expression levels of cortactin, a gene in the 11q13 amplicon. *Oncogene* 28, 431-444 (2009)

57. Paterson AL, JC Pole, KA Blood, MJ Garcia, SL Cooke, AE Teschendorff, Y Wang, SF Chin, B Ylstra, C Caldas, PA Edwards: Co-amplification of 8p12 and 11q13 in breast cancers is not the result of a single genomic event. *Genes Chromosomes Cancer* 46, 427-439 (2007)

58. Tornillo L, G Duchini, V Carafa, A Lugli, S Dirnhofer, D Di Vizio, A Boscaino, R Russo, C Tapia, R Schneider-Stock, G Sauter, L Insabato, LM Terracciano: Patterns of gene amplification in gastrointestinal stromal tumors (GIST). *Lab Invest* 85, 921-931 (2005)

59. Coon JS, E Marcus, S Gupta-Burt, S Seelig, K Jacobson, S Chen, V Renta, G Fronda, HD Preisler: Amplification and overexpression of topoisomerase IIalpha predict response to anthracycline-based therapy in locally advanced breast cancer. *Clin Cancer Res* 8, 1061-1067 (2002)

60. Yarden Y, MX Sliwkowski: Untangling the ErbB signalling network. *Nat Rev Mol Cell Biol* 2, 127-137 (2001)

61. Mocanu MM, Z Fazekas, M Petras, P Nagy, Z Sebestyen, J Isola, J Timar, JW Park, G Vereb, J Szollosi: Associations of ErbB2, beta1-integrin and lipid rafts on

Herceptin (Trastuzumab) resistant and sensitive tumor cell lines. *Cancer Lett* 227, 201-212 (2005)

62. Palyi-Krekk Z, M Barok, J Isola, M Tammi, J Szollo si, P Nagy: Hyaluronan-induced masking of ErbB2 and CD44-enhanced trastuzumab internalisation in trastuzumab resistant breast cancer. *Eur J Cancer* 43, 2423-2433 (2007)

63. Palyi-Krekk Z, M Barok, T Kovacs, H Saya, O Nagano, J Szollosi, P Nagy: EGFR and ErbB2 are functionally coupled to CD44 and regulate shedding, internalization and motogenic effect of CD44. *Cancer Lett* 263, 231-242 (2008)

64. Fazekas Z, M Petras, A Fabian, Z Palyi-Krekk, P Nagy, S Damjanovich, G Vereb, J Szollosi: Two-sided fluorescence resonance energy transfer for assessing molecular interactions of up to three distinct species in confocal microscopy. *Cytometry A* 73, 209-219 (2008)

65. Barok M, M Balazs, P Nagy, Z Rakosy, A Treszl, E Toth, I Juhasz, JW Park, J Isola, G Vereb, J Szollosi: Trastuzumab decreases the number of circulating and disseminated tumor cells despite trastuzumab resistance of the primary tumor. *Cancer Lett* 260, 198-208 (2008)

66. Osta WA, Y Chen, K Mikhitarian, M Mitas, M Salem, YA Hannun, DJ Cole, WE Gillanders: EpCAM is overexpressed in breast cancer and is a potential target for breast cancer gene therapy. *Cancer Res* 64, 5818-5824 (2004)

67. Spizzo G, G Gastl, D Wolf, E Gunsilius, M Steurer, D Fong, A Amberger, R Margreiter, P Obrist: Correlation of COX-2 and Ep-CAM overexpression in human invasive breast cancer and its impact on survival. *Br J Cancer* 88, 574-578 (2003)

68. Al-Hajj M, MS Wicha, A Benito-Hernandez, SJ Morrison, MF Clarke: Prospective identification of tumorigenic breast cancer cells. *Proc Natl Acad Sci U S A* 100, 3983-3988 (2003)

69. Fabian A, M Barok, G Vereb, J Szollosi: Die hard: are cancer stem cells the Bruce Willises of tumor biology? *Cytometry A* 75, 67-74 (2009)

**Abbreviations:** aCGH: array comparative genomic hybridization; cCGH: chromosomal comparative genomic hybridization; FISH: fluorescence *in situ* hybridization; SCID: severe combined immunodeficiency disease; BAC: bacterial artificial chromosome; IgG: immunoglobulin G; GAMIG: goat-anti-mouse immunoglobulin G*;* ESA: epithelial specific antigen; RTKs: receptor tyrosine kinases; mAb: monoclonal antibody*;* EGF: Epidermal Growth Factor; ADCC: antibody-dependent cellular cytotoxicitiy;

**Key Words:** Drug Resistance, Trastuzumab, Breast Tumor Xenograft, ErbB2/HER-2, array-CGH, Gene And Protein Expression

**Send correspondence to:** Margit Balazs, Division of Biomarker Analysis, Department of Preventive Medicine, Faculty of Public Health , Medical and Health Science Center, University of Debrecen, 4028 Debrecen Kassai str. 26/b, Hungary, Tel: 36-52-460-190/77151, Fax: 36-52-417-267, E-mail:margo@med.unideb.hu

http://www.bioscience.org/current/vol2E.htm